Since January 2020 Elsevier has created a COVID-19 resource centre with free information in English and Mandarin on the novel coronavirus COVID-19. The COVID-19 resource centre is hosted on Elsevier Connect, the company's public news and information website.

Journal of Immunological Methods 368 (2011) 24–35

Contents lists available at ScienceDirect

Journal of Immunological Methods

journal homepage: www.elsevier.com/locate/jim

Research paper

Validation of assays to monitor immune responses in the Syrian golden hamster (*Mesocricetus auratus*)

Marko Zivcec [a,b], David Safronetz [a], Elaine Haddock [a], Heinz Feldmann [a,b,*], Hideki Ebihara [a,**]

[a] Laboratory of Virology, Division of Intramural Research, National Institute of Allergy and Infectious Diseases, National Institutes of Health, Rocky Mountain Laboratories, 903 S 4th Street, Hamilton, MT, USA

[b] Department of Medical Microbiology and Infectious Disease, University of Manitoba, 745 Bannatyne Avenue, Winnipeg, Manitoba, Canada

ARTICLE INFO

Article history:
Received 28 October 2010
Received in revised form 7 February 2011
Accepted 8 February 2011
Available online 17 February 2011

Keywords:
Syrian Golden hamster
qRT-PCR
Host immune response
Reference genes

ABSTRACT

The Syrian golden hamster (*Mesocricetus auratus*) is a valuable but under-utilized animal model for studies of human viral pathogens such as bunyaviruses, arenaviruses, flaviviruses, henipaviruses, and SARS-coronavirus. A lack of suitable reagents and specific assays for monitoring host responses has limited the use of this animal model to clinical observations, pathology and humoral immune responses. The objective of this study was to establish and validate assays to monitor host immune responses in the hamster including important pro-inflammatory, anti-inflammatory and innate immune responses, as well as markers of apoptosis, cell proliferation, cell junction integrity and coagulation. Commercially available mouse and rat ELISA and luminex panels were screened for potential cross-reactivity, but were found to be of limited value for studying host responses in hamsters. Subsequently, quantitative reverse transcriptase polymerase chain reaction (qRT-PCR) assays for the detection of 51 immune-related and four internal reference genes were developed. To validate the immune-related assays, hamsters were infected with vesicular stomatitis virus (VSV), Indiana species, or treated with lipopolysaccharide (LPS) and host immune responses were monitored in selected organs. Ribosomal protein L18 was identified as the most stable internal reference gene. In conclusion, these new assays will greatly improve the use of the hamster as an important small animal model in infectious disease research.

Published by Elsevier B.V.

1. Introduction

Syrian golden hamsters (*Mesocricetus auratus*; hereafter referred to as hamster) have been used in numerous studies as infection and disease models (Table 1) due to their ease of handling and disease development, which often mimics the natural course of human diseases. In particular, hamsters have been recognized as valuable animal models for studying emerging and high consequence acute human viral diseases caused by bunyaviruses (Niklasson et al., 1984; Hooper et al., 2001; Milazzo et al., 2002; Fisher et al., 2003) arenaviruses (Smee et al., 1993; Sbrana et al., 2006), henipaviruses (Wong et al., 2003), flaviviruses (Tesh et al., 2001; Xiao et al., 2001; Siirin et al., 2007) and SARS-coronavirus (Roberts et al., 2005). For some of these pathogens, such as Andes virus, a New World hantavirus and a causative agent of hantavirus pulmonary syndrome, hamsters are the only lethal disease model (Hooper et al., 2001). However, due to a lack of available reagents and specific assays to monitor host responses in hamsters, including disease-decisive acute and early innate immune responses, investigators are currently limited to studies on disease progression (clinical symptoms),

Abbreviations: β2M, Beta-2-microglobulin; BBQ, Blackberry quencher; HPRT, Hypoxanthine phosphoribosyltransferase; LPS, Lipopolysaccharide; RPL18, Ribosomal protein L18; VSV, vesicular stomatitis Indiana virus; Yak, Yakima yellow.

* Correspondence to: H. Feldmann, Laboratory of Virology, Division of Intramural Research, National Institute of Allergy and Infectious Diseases, National Institutes of Health, Rocky Mountain Laboratories, 903 S 4th Street, Hamilton, MT, USA Tel.: +1 406 375 7410; fax: +1 406 375 7416.

** Corresponding author. Tel.: +1 406 375 7419; fax: +1 406 375 9620.

E-mail addresses: feldmannh@niaid.nih.gov (H. Feldmann), ebiharah@niaid.nih.gov (H. Ebihara).

0022-1759/$ – see front matter. Published by Elsevier B.V.
doi:10.1016/j.jim.2011.02.004

Table 1
Selected biological agent disease models in Syrian Golden hamsters.

Agent	Disease modeled	Reference
Amebic liver abscess	Entamoeba histolytica	Ghadirian et al., 1980
Andes virus	Hantavirus pulmonary syndrome	Hooper et al., 2001
Babesia	Babesiosis	Braga et al., 2006
Eastern equine encephalitis virus	Eastern equine encephalitis	Paessler et al., 2004
Gabek Forest virus	Rift Valley fever-like [a]	Fisher et al., 2003
Japanese encephalitis virus	Japanese encephalitis	Larson et al., 1980
Leishmania	Visceral leishmania	Melby et al., 2001
Leptospira	Leptospirosis	Haake, 2006
Maporal virus	Hantavirus pulmonary syndrome	Milazzo et al., 2002
Nipah virus	Nipah virus encephalitis	Wong et al., 2003
Oncolytic adenoviruses	Pancreatic carcinoma	Spencer et al., 2009
Pichinde virus	Lassa fever-like	Smee et al., 1993
Pirital virus	Lassa fever-like	Sbrana et al., 2006
Prions	Scrapie, Creutzfeldt–Jakob disease	Beekes et al., 1996; Chabry et al., 1999
Punta Tora virus	Rift Valley fever-like	Fisher et al., 2003
Rift Valley virus	Rift Valley fever	Niklasson et al., 1984
St. Louis encephalitis virus	Chronic St. Louis encephalitis [a]	Siirin et al., 2007
SARS coronavirus	Severe acute respiratory syndrome [a]	Roberts et al., 2005
Venezuelan equine encephalitis virus	Venezuelan equine encephalitis**	Jackson et al., 1991
West Nile virus	West Nile neurological syndrome	Xiao et al., 2001
Western equine encephalitis virus	Western equine encephalitis	Zlotnik et al., 1972
Yellow fever virus [b]	Yellow fever	Tesh et al., 2001

[a] Infection model, not disease model.
[b] Adapted viruses used in model.

humoral immune responses (antibodies) and pathology. For other disease models using rodents, nonhuman primates and ferrets, expression microarray proteome and luminex technology-based quantification assays have been developed and utilized (Kayo et al., 2001; Datson et al., 2007; Bruder et al., 2010; Ierna et al., 2010). However, for Syrian (Golden) hamsters similar specific assays are not available due to the lack of a complete genome sequence.

Here, we describe the testing of a large panel of ELISA and luminex based assays for cross-reactivity against hamster proteins and the development of an extended panel of real-time quantitative reverse transcriptase polymerase chain reaction (qRT-PCR) assays which were based on hamster mRNA sequences currently registered in Genbank. Due to limited cross-reactivity in ELISA and luminex based assays, the development of qRT-PCR assays seemed the most practical and useful strategy to quantify specific host responses in the hamster model. A few qRT-PCR assays for the quantification of a limited number of immunological responses have been previously reported (Melby et al., 1998; Muller et al., 2001; Vernel-Pauillac and Merien, 2006). We developed a unique extended panel of TaqMan® primer/probe assays for 51 different genes targeting specific markers in the pro-inflammatory, anti-inflammatory, innate immunity, apoptosis, cell junction and coagulation responses of the hamster. With ribosomal protein L18 we identified a more suitable and stable housekeeping gene. The assays were validated by monitoring host responses to treatment with lipopolysaccharide (LPS) and infection with vesicular stomatitis Indiana virus (VSV), both of which are known to strongly activate host responses in the hamster (Fultz et al., 1981b; Muller et al., 2001). The new assays will allow for a broader monitoring of host responses against infection and an advanced utilization of the hamster model.

2. Materials and methods

2.1. Inoculations and sample preparation

Recombinant VSV was rescued from cloned cDNA and infectivity was titered by conventional plaque forming assay, as described previously (Lawson et al., 1995; Garbutt et al., 2004). Three groups of six hamsters (female, 4–6 weeks old Harlan Laboratories Inc, Indianapolis, IN, USA) were injected intraperitoneally (ip) with either 50 μg LPS (Sigma, St. Louis, MO USA), 10^6 plaque forming units (pfu) of VSV (both diluted in Dulbecco's modified Eagle's medium (DMEM)), or DMEM only (control) in a total volume of 400 μL. Three of the controls and VSV infected, and six of the LPS treated hamsters were euthanized by exsanguination while under deep anesthesia (inhalational isoflurane) one day post inoculation. The remaining control and VSV inoculated hamsters were euthanized at 3 days post inoculation. Whole blood was collected by cardiac puncture into EDTA vacutainers, after which plasma was separated by centrifugation and frozen at −80 °C. Lung, liver and spleen samples were harvested from euthanized hamsters, cut into approximately 50–100 mg pieces and submerged in 1 mL of RNAlater (Qiagen, Valencia, CA, USA) overnight at 4 °C. The following day RNAlater was removed and the tissues were frozen at −80 °C. Approximately 30 mg of the tissue samples were mechanically homogenized in RLT buffer and the RNA was extracted from the homogenate using the RNeasy Mini Kit (Qiagen) according to the manufacturer's instructions. The concentration of the extracted RNA was determined using a NanoDrop 8000 instrument (Thermo Scientific, Waltham, MA, USA) and adjusted to a final concentration of 10 ng/μL. All experiments were conducted under BSL2 conditions, and approval for animal experiments was obtained from the Institutional Animal Care and Use Committee. Animal work was performed by certified staff in a facility approved by the Association for Assessment and Accreditation of Laboratory Animal Care.

2.2. ELISA and Milliplex panel preparation

Rat TNFα, IL-2, IL-6 and IL-10, mouse CXCL10/IP-10, IL-13 and IL-1β/IL-1F2, and mouse/rat/porcine/canine TGFβ1 ELISA kits were purchased from R&D Systems (Minneapolis, MN, USA) and tested according to manufacturer's instructions with individual hamster plasma (Table 2). Individual control and VSV infected and pooled LPS hamster plasma were sent to Millipore (Billerica, MA, USA) for analysis by Milliplex® MAP Mouse (32 plex) and Rat (23 plex) Cytokine panels (Table 2).

Table 2
List of commercially available, rodent specific, ELISA and Luminex based assays examined for cross-reactivity with hamster proteins. Red indicates acceptable cross-reactivity (within the range of supplied standards), orange indicates marginal cross-reactivity (low or suspiciously high concentrations detected) and blue indicates no cross-reactivity.

R&D Systems ELISA	Rat	TGFβ	IL-10	TNFα	IL-2	IL-6	
	Mouse	IL-1β	IP-10	IL-13			
Millipore Luminex Panels	Rat	Eotaxin	GM-CSF	G-CSF	MCP-1	LEPTIN	MIP-1α
	Rat	GRO/KC	IFNγ	TNFα	IP-10	RANTES	VEGF
	Rat	IL-1α	IL-1β	IL-2	IL-4	IL-5	IL-6
	Rat	IL-10	IL-12p70	IL-13	IL-17	IL-18	
	Mouse	Eotaxin	GM-CSF	G-CSF	MCP-1	M-CSF	MIP-1α
	Mouse	MIP-1β	IFNγ	TNFα	IP-10	RANTES	VEGF
	Mouse	MIP-2	KC	LIF	LIX	MIG	IL-1α
	Mouse	IL-1β	IL-2	IL-3	IL-4	IL-5	IL-6
	Mouse	IL-7	IL-9	IL-10	IL-12p40	IL-12p70	IL-13
	Mouse	IL-15	IL-17				

2.3. Selection of target genes for development qRT-PCR assay

Over 800 hamster mRNA sequences have been registered in Genbank. Of those, 51 target genes related to host immunological responses elicited by pathogen infections were selected. These included pro-inflammatory, anti-inflammatory, innate immune (primarily Type I IFN-relating genes), and T-cell-mediated responses, as well as apoptosis, cell junctions and coagulation markers (Table 3) (Adler, 2008).

2.4. Internal control selection

Of the available hamster sequences on Genbank, the following four "housekeeping" genes were selected as internal reference genes: Hypoxanthine phosphoribosyltransferase (HPRT), β-actin, β-2-microglobulin (β2M) and ribosomal protein L18 (RPL18). β-actin and HPRT were chosen as these are seen as classical housekeeping genes and have been previously utilized by other researchers performing quantitative RT-PCR on hamster tissues (Melby et al., 1998). β2M and RPL18 were selected based on the work of Dheda et al. (2004). All 4 genes were tested in qRT-PCR experiments to determine which had the most stable expression in the tissues of infected/treated and control hamsters.

2.5. Primers and probes

qRT-PCR primers and probes were either designed with the aid of Primer Express® Software v3.0 (Applied Biosystems, Foster City, CA, USA), or were directly designed and synthesized by TIB MOLBIOL (Adelphia, NJ, USA) based on the sequence information of target transcripts. Sequence information of primers and probes are shown in Table 3. Prior to use in qRT-PCR assays all the primer sets were tested to ensure the primers can amplify target transcripts by conventional reverse transcriptase PCR; amplicons were analyzed by agarose gel electrophoresis. Briefly, using Superscript III Reverse Transcriptase (Invitrogen, Carlsbad, CA, USA) and random hexamers, cDNA pools were generated according to manufacturer's instructions from RNA derived from hamster spleen, lung or liver. The cDNA was used as template for conventional PCR. All PCR reactions were carried out using Taq polymerase (Qiagen Cat. No. 201203) at a denaturation temperature of 95 °C for 30 s, annealing temperature of 50 °C for 30 s, and an extension temperature of 72 °C with an extension time of 30 s for 40 cycles. If a band was evident at the correct size on an agarose gel, the primers were used for subsequent qRT-PCR runs. In total, 51 different primer/probe sets were validated on lung, liver and spleen tissues (Table 3). All experimental gene probes were labeled with 5′ 6FAM dye and quenched by 3′ BlackBerry Quencher (BBQ), and all internal control gene probes were labeled with Yakima Yellow (Yak) and quenched by BBQ (TIB MOLBIOL).

2.6. Primer and probe efficiency and limit of detection

The limit of detection and efficiency of cDNA amplification was determined by selecting a few representative cloned genes. The clones were altered to contain a T7 promoter directly upstream to the qRT-PCR forward primer binding site. Following amplification the PCR fragments were gel purified and *in vitro* transcribed by Riboprobe Combination System T3/T7 RNA Polymerase (Promega, Madison, WI, USA). Transcripts were DNase I digested and the RNA purified using TRIzol reagent (Invitrogen) according to manufacturer's instructions. The purified RNA was diluted from 5×10^{1} to 5×10^{-8} ng RNA and used as a template for qRT-PCR reactions. To determine the minimum amount of total hamster tissue RNA required for the experiments, representative genes were selected and run in a 2-fold dilution series (from 200 ng to 50 ng total RNA per reaction).

To test whether the efficiency of the primer/probe sets was suitable for direct comparison between reactions, approximately one third of the available genes were selected and cloned into pCR2.1-TOPO (Invitrogen) according to the manufacturer's instructions. The inserts were verified by sequencing and entire plasmids were diluted in series of $\log_{10}$ from 5×10^{1} to 5×10^{-9} ng of total DNA. Quantitative PCR and qRT-PCR were carried out on the plasmid and RNA dilution series, respectively, and the crossing threshold (C_T) values plotted and efficiency determined by measuring the slope of the best fit line through the C_T values. If the efficiencies were within 10% of each other the primer/probe sets were considered as being comparable (Ling et al., 2008).

2.7. qRT-PCR methods

All qRT-PCR experiments were performed on the Rotor-Gene 6000 thermal cycler (Corbett, San Francisco, CA, USA) using Rotor-Gene Probe RT-PCR kits (Qiagen) according to manufacturer's instructions. Each reaction was multiplexed with RPL18 as the internal reference, using 50 ng of template RNA. The final concentration of each test primer and probe set was 0.4 μM and 0.1 μM, respectively. The final concentration

Table 3
Detailed sequence information of the primers and probes utilized in these studies. Primers and probes for the indicated genes were designed based on Syrian golden hamster specific sequences available on GenBank (accession number provided in brackets). The melting temperature of all these primers was ~55 °C and the melting point of the probes was ~65 °C.

β-2-Microglobulin	B2M F	GGCTCACAGGGAGTTTGTAC	Fibrinogen A α- chain (D43757)	FAAC F	GCACAAGCACGACACGT
(X17002)	B2M R	TGGGCTCCTTCAGAGTTATG		FAAC R	TGGGTCATGCCTAAGTCTCC
	B2M TM	YAK-CTGCGACTGATAAATACGCCTGCA-BBQ		FAAC TM	6FAM-CGATGGTCACCGAGAAGTGGTCA-BBQ
β-actin	bactin F	ACTGCCGCATCCTCTTCCT	Forkhead box P3 (FJ664148)	FbP3 F	AAGCAGATCACCTCCTGGAT
(AJ312092)	bactin R	TCGTTGCCAATGGTGATGAC		FbP3 R	AGCTGCTGCTCCAGAGAC
	bactin TM	6FAM-CCTGGAGAAGAGCTATGAGCTGCCTGATG-BBQ		FbP3 TM	6FAM-CACCACTTCTCTCTGGAGGAGGCAC-BBQ
B-cell lymphoma 2	Bcl2 F	CTTCGCAGAGATGTCCAGTC	Hypoxanthine phosphoribosyltransferase	HPRT F	TGCGGATGATATCTCAACTTTAACTG
protein (bcl-2) (AJ582074)	Bcl2 R	CATCTCCCTGTTGACGCTC	(AF047041)	HPRT R	AAAGGAAAGCAAAGTTTGTATTGTCA
	Bcl2 TM	6FAM-TGACGCCCTTCACCGCGA-BBQ		HPRT TM	6FAM-AAAGAATGTCTTGATTGTTGAAGGTAAAACTGACATTGG-BBQ
Bcl-2 associated protein	Bax F	GGCAACTTCAACTGGGG	Inducible nitric oxide synthase-2	iNOS F	TGGCAGGATGGGAAACTGA
(AJ582075)	Bax R	CCACCCTGGTCTTGGATC	(AY297461)	iNOS R	GCACCGCTTTCACCAAGACT
	Bax TM	6FAM-CCAGCCCATGATGGTTCTGATTAGC-BBQ		iNOS TM	6FAM-CCCAGGAGGAGAGAGATCCGGCTC-BBQ
CD83 protein DQ094177	CD83 F	AACCTGGTACGGAACAAGCT	Intracellular adhesion molecule-1	ICAM1 F	TGCAGCCGGAGAACAGATG
	CD83 R	CAAAGGAAGGTTGCCGTC	(DQ093373)	ICAM1 R	ATCTCCCGTGTGACAGTCTTCA
	CD83 TM	6FAM-TCCAGGCAGCATTCAGGTACACTGA-BBQ		ICAM1 TM	6FAM-AGCCCTCGCTGCCCATCGGG-BBQ
Chemokine (C-X-C motif) ligand	IP-10F	GCCATTCATCCACAGTTGACA	Interferon-α inducible protein	p27 F	TCGTTGCTGCTCCCGTAGTC
10 (IP-10) (AY007988)	IP-10 R	CATGGTGCTGACAGTGGAGTCT	(p27-h) (AF212039)	p27 R	ATGGATCCCGCTGCAATTC
	IP-10 TM	6FAM-CGTCCCGAGCCAGCCAACGA-BBQ		p27 TM	6FAM-TGGGTGCTGTGGGCTTCACTGG-BBQ
Chemokine CCL20/MIP-3 α	CCL20 F	AGTCAGTCAGAAGCAAGCAACT	Interferon-γ (AF034482)	IFNg F	GGCCATCCAGAGGAGCATAG
(AY924377)	CCL20 R	TGAAGCGGTGCATGATCC		IFNg R	TTTCTCCATGCTGCTGTTGAA
	CCL20 TM	6FAM-CACAAGGAGCACTATCCCACCCAGA-BBQ		IFNg TM	6FAM-CACCATCAAGGCAGACCTGTTTGCTAACTT-BBQ
Chemokine ligand 17 (FJ664143)	CL17 F	CGAGTGCTGCCTGGAGATC	Interferon regulatory factor-1	IRF1 F	GGCATACAACATGTCTTCACG
	CL17 R	TGATGGCCTTCTTCACATGC	(DQ092344)	IRF1 R	GCTATGCTTTGCCATGTCAA
	CL17 TM	6FAM-TGGACCTGCCCTGGACAGTCACA-BBQ		IRF1 TM	6FAM-CACAATGACGCCAGACCTTGCTCA-BBQ
Chemokine ligand 22 (FJ664144)	CL22 F	CGCGTAGTGAAGGAGTTCTTC	Interferon regulatory factor-2	IRF2 F	AATGCCTTCAGAGTGTACCG
	CL22 R	TCTTCACCAGGCCAGCTTA	(AY714581)	IRF2 R	TGTTCACCGTACTATCCACTTCAT
	CL22 TM	6FAM-ACCTCAAAGTCCTGCCGCAAGCC-BBQ		IRF2 TM	6FAM-CTGAAGTCAGGACCGCATACTCAGGA-BBQ
Claudulin-1 (EU856105)	ham cld1 F2	GCCACAGCATGGTATGGAA	Interleukin-1β (AB028497)	IL-1b F	GGCTGATGCTCCCATTCG
	ham cld1 R1	GCAAGAAAGTAGGGCACCTC		IL-1b R	CACGAGGCATTTCTGTTGTTCA
	ham cld1 TM	6FAM- CCCGTCAATGCCAGGTATGAATT-BBQ		IL-1b TM	6FAM-CAGCTGCACTGCAGGCTCCGAG-BBQ
Complement C3 (complement C3d region)	CC3d F	GGAGCCTTACCTCAGCAAGT	Interleukin-2 (EU729351)	IL-2F	GTGCACCCACTTCAAGCTCTAA
(AB024425)	CC3d R	TAGCCGCCTCCGTAGTATCT		IL-2 R	AAGCTCCTGTAAGTCCAGCAGTAAC
	CC3d TM	6FAM-CAGAAGCTCTACAATGTGGAGGCCA-BBQ		IL-2 TM	6FAM-AGGAAACCCAGCAGCACCTCGAGC-BBQ
Complement component 5 (DQ369042)	CC5 F	GTAGTTCCCGATGCTGAAGTG	Interleukin-4 (AF046213)	IL-4F	CCACGGAGAAAGACCTCATCTG
	CC5 R	TGATTAACTCCATTGACCAACG		IL-4 R	GGGTCACCTCATGTTGGAAATAAA
	CC5 TM	6FAM-TGTGACTTGCATCGCTTTCGGC-BBQ		IL-4 TM	6FAM-CAGGGCTTCCCAGGTGCTTCGCAAGT-BBQ
Complement protein C1qBP	CP1qBP F	CAGAGGATGAGGTTGGACAA	Interleukin-6 (AB028635)	IL-6F	CCTGAAAGCACTTGAAGAATTCC
(DQ367730)	CP1qBP R	CCATTAGGTGGTCATACAAGGC		IL-6 R	GGTATGCTAAGGCACAGCACACT
	CP1qBP TM	6FAM-TCCATTCAGAGTCACCAGTGGTCTGGA-BBQ		IL-6 TM	6FAM-AGAAGTCACCATGAGGTCTACTCGGCAAAA-BBQ
E-cadherin (DQ237892)	Ecad F	GTTAAGGTTCTGGAGATGAGATTGG	Interleukin-10 (AF046210)	IL-10F	GTTGCCAAACCTTATCAGAAATGA
	Ecad R	CATCTTTCCCCTCCGAGACA		IL-10 R	TTCTGGCCCGTGGTTCTCT
	Ecad TM	6FAM-TTATGTAGATGACCATGACTTTAATGACAA-BBQ		IL-10 TM	6FAM-CAGTTTTACCTGGTAGAAGTGATGCCCCAGG-BBQ
Epithelial mucin (Muc1) (L41545)	Muc1 F	CGGAAGAACTATGGGCAGCT	Interleukin-12 p35 subunit (AB085791)	IL-12p35 F	GGCCTTCCCTGGCAGAA
	Muc 1 R	GCCACTACTGGGTTGGTGTAAG		IL-12p35 R	ATGCTGAAAGCCTGCAGTAGAAT
	Muc 1 TM	6FAM-TGCCTGCCGAGACCTCCTCGTA-BBQ		IL-12p35 TM	6FAM-CGGATCCCTACAAAGTGAAAATGAAGCTCTG-BBQ

(continued on next page)

Table 1 *(continued)*

Interleukin-12 p40 subunit (AB085792)	IL12p40 F	TGGTTACCTCCTTAGCAGTCC	Signal transducer and activator of transcription-1 β (AB177397)	STAT1b F	AGGTCCGTCAGCAGCTTAA
	IL12p40 R	TCAGCCTGATGATGAACCTGA		STAT1b R	GCCGTTCCACCACAAAT
	IL12p40 TM	6FAM-TCCAGAGTGCCATAATAGCCACACAAA-BBQ		STAT1b TM	6FAM-TCTGAATGAGCTGCTGGAAGAGGACA-BBQ
Interleukin-21 (FJ664142)	IL21 F	TCAACTGATGTGAAAGGAGC	Signal transducer and activator of transcription-2 (AB177399)	STAT2 F	AATGCCTTCAGAGTGTACCG
	IL21 R	ATCTTGTGGAGCTGGCAG		STAT2 R	TGTTCACCGTACTATCCACTTCAT
	IL21 TM	6FAM-TCAGGGTCCTAGCCAAAAGAGAATC-BBQ		STAT2 TM	6FAM-CTGAAGTCAGGACCGCATACTCAGGA-BBQ
Interleukin-2 receptor-α (DQ093372)	IL2Ra F	AAAGCAAGCTACACCTAACCC	Tight junction protein 2 (EU856099)	ham tjp2 F1	CTACACTGACAATGAGCTGGA
	IL2Ra R	GCCTTGTATCCTTGAATGCG		ham tjp2 R1	CTCTGGGCTGGATTTCCTTA
	IL2Ra TM	6FAM-CAGAAATCAGCACAGTCTGTGCACCA-BBQ		ham tjp2 TM	6FAM-TCATGCTGCACCGGCTCCGA-BBQ
Interleukin-6 signal transducer (EF442778)	IL6ST F	TGAAGATACAGCATCTTCCCG	Tissue inhibitor of matrix metalloproteinase-2 (AF260255)	TIMM2 F	AGAGCCTGAACCACAGGT
	IL6ST R	TGAAGATACAGCATCTTCCCG		TIMM2 R	CGGGTCCTCGATGTCAA
	IL6ST TM	6FAM-TCACTCCAGTAGCCTTTGCCATCCT-BBQ		TIMM2 TM	6FAM-CGAGTGCAAGATCACACGCTGCC-BBQ
Junction adhesion molecule (EU856104)	ham jam F1	CGTCCAAGTTCCCGAGAGTA	Transforming growth factor-β1 (AF046214)	TGFb F	TGTGTGCGGCAGCTGTACA
	ham jam R1	CGTGATCTGGCTGTTATAGCA		TGFb R	TGGGCTCGTGAATCCACTTC
	ham jam TM	6FAM-TAGTGCCACCCTGGACGAACTTC-BBQ		TGFb TM	6FAM-CGACTTTCGCAAGGACCTGGGCT-BBQ
Matrix metalloproteinase-2 (AF260254)	MM2 F	GATGCTGCCTTTAACTGGAGT	Transforming growth factor 2 (AY007214)	TGFb2 F	TGCTGCCCTCCTACAGACT
	MM2 R	GAGCTTAGGGAAACCAGGAT		TGFb2 R	GCACAGAAGTTGGCATTATACC
	MM2 TM	6FAM-CATACATCTTCGCTGGAGACAAGTTC-BBQ		TGFb2 TM	6FAM-CACAACAGTCCAATCGGCGGA-BBQ
MHC class II antigen alpha chain (DQ092501)	MHCAAC F1	CAGGGAGGACTGCAAGCTATA	Transforming growth factor-β 3 (AF298188)	TGFb3 F	CAAGCTCAGGCTCACCAGT
	MHCAAC R	TGTCCACGAAGCAGATGAG		TGFb3 R	CCGACTCTGTGTTCTCCTGAG
	MHCAAC TM	6FAM-TGCAGCAAAGCAGAACTTGGACATC-BBQ		TGFb3 TM	6FAM-AGCCATCGGTGATGACCCACGT-BBQ
Myxovirus resistance protein-2 (EU616539)	Mx2 F	CCAGTAATGTGGACATTGCC	Transforming growth factor-β type I receptor (AF298187)	TGFbTIR F	ATCAAACTTGCTCTGTCTACGG
	Mx2 R	CATCAACGACCTTGTCTTCAGTA		TGFbTIR R	TGTCTGTGGCAGAATCATGC
	Mx2 TM	6FAM-TGTCCACCAGATCAGGCTTGGTCA-BBQ		TGFbTIR TM	6FAM-ACAGCCAGTCCCAAGTCTGCAATAC-BBQ
Nitric oxide synthase-2 (DQ355357)	NOS2 F	TGCCTTGCATCCTCATTGG	Tumor Necrosis Factor-α (AF315292)	TNFa F	GGAGTGGCTGAGCCATCGT
	NOS2 R	GTCGCTGTTGCCAGAAACTG		TNFa R	AGCTGGTTGTCTTTGAGAGACATG
	NOS2 TM	6FAM-CCTGGCACGGGCATCGCTC-BBQ		TNFa TM	6FAM-CCAATGCCCTCCTGGCCAACG-BBQ
Occuldin (EU856106)	ham occ F1	CTATTCTGGGCATCCTGGT	Vascular endothelial growth factor (AF297627)	VEGF F	CAGGAGTACCCCGATGAGATAGA
	ham occ R1	TTGCACATGGCATAGATCTG		VEGF R	CCCCCACACCGCATCA
	ham occ TM	6FAM- AGTCAACCCAACTGCCCAGGCT-BBQ		VEGF TM	6FAM-TCTTCAAGCCGTCCTGTGTGCCC-BBQ
p75 tumor necrosis factor membrane receptor (AF315291)	p75 F	CCCCAGGCCACAGTCAC			
	p75 R	GCCGTGGGAGGAATCTGAA			
	p75 TM	6FAM-CTGCACAGGCCTCCTGAGACCCT-BBQ			
Platelet endothelial adhesion molecule (AF508040)	PECAMF	CAGGATCAGAACTTCAGCAAGAT			
	PECAMR	GCAGCTGATGGTTATAGCATGT			
	PECAM TM	6FAM-TGTACCGCAGGCATCGGCAGA-BBQ			
Protein kinase R (DQ645944)	Eif2ak2 F	ACGGACCTAAGAGATGGCAT			
	Eif2ak2 R	AGGTAACTAAAGCGGAGTGC			
	Eif2ak2 TM	6FAM-CCACGGATCGACCTAGTGCTTCTGA-BBQ			
Ribosomal Protein L 18 (DQ403027)	RPL18 F	GTTTATGAGTCGCACTAACCG			
	RPL18 R	TGTTCTCTCGGCCAGGAA			
	RPL18 TM	YAK-TCTGTCCCTGTCCCGGATGATC-BBQ			
Signal transducer and activator of transcription-1 (DQ092343)	STAT1 F	GCCAACGATGATTCCTTTGC			
	STAT1 R	GCTATATTGGTCATCCAGCTGAGA			
	STAT1 TM	6FAM-ACCATCCGTTTCCATGACCTCC-BBQ			

of the internal control primer and probe set was 0.2 μM and 0.05 μM, respectively. Cycling conditions were as follows: 10 min at 50 °C (initial reverse transcription), 5 min at 95 °C (denaturation and HotStarTaq activation), and 40 cycles of 5 s at 95 °C (denaturation), followed by 10 s at 60 °C per cycle (annealing/amplification). Data acquisition was carried out at the end of the annealing/amplification step in the green (510 nm) and yellow (555 nm) channels.

2.8. Data analysis

The data were analyzed using the ΔΔCT method (Livak and Schmittgen, 2001). Briefly, the C_T of each test gene in a treated hamster was first normalized to the RPL18 C_T (ΔCT) and then compared to the same normalized gene in a mock-treated (calibrator) hamster to determine the ΔΔCT. The final value is displayed as the relative fold increase between the infected/treated and mock treated hamsters.

3. Results and discussion

3.1. Examination of cross-reactivities of ELISA and luminex based cytokine/chemokine detection assays

Many important genes are highly conserved between species; therefore cross-reactivity of antibodies isolated against other rodents may detect hamster proteins. First, we compared amino acid sequence homologies of representative cytokines and chemokines between hamsters, rats, and mice. We selected target proteins showing >90% homology at the amino acid level (data not shown) and tested cross-reactivities of ELISA kits for their detection. In total 63 antibody-based (55 luminex, 8 ELISA) assays were tested for cross-reactivity with hamster proteins and only 14 were determined to display cross-reactivity (Table 2). The mouse and rat ELISA kits tested in this study had limited cross-reactivity with hamster proteins. Of the eight ELISA kits tested, only three (mouse IL-1β, rat IL-10 and rat/mouse/porcine/canine TGFβ1) displayed cross-reactivity against the

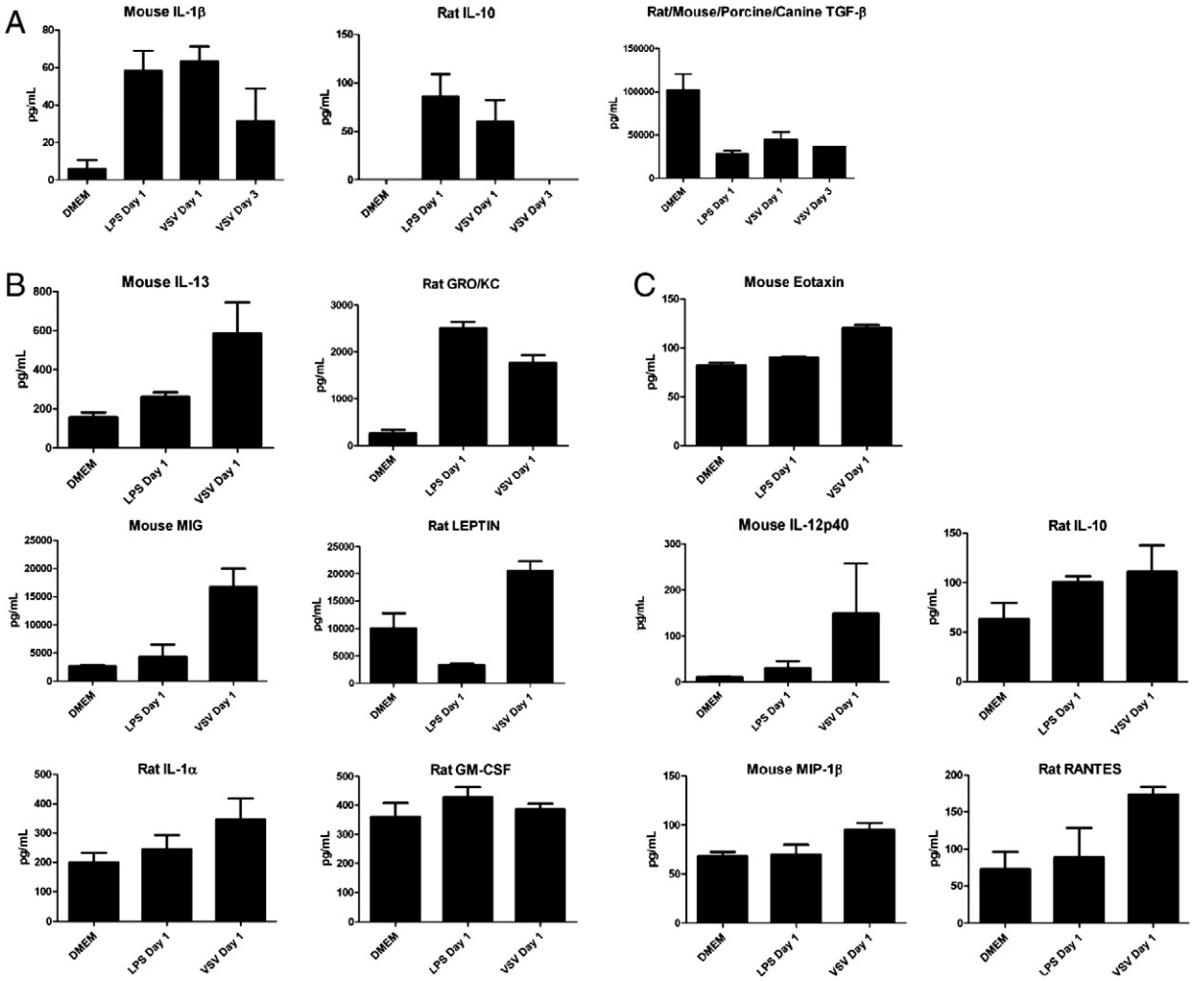

Fig. 1. Evaluation of commercially available, rodent specific, ELISA and Luminex based assays for the detection of hamster homologues. (A) ELISA based cross-reactivity data for IL-1β, IL-10 and TGFβ. Luminex based cross-reactivity data displaying (B) acceptable and (C) marginal cross reactivity between mouse and rat homologues. Error bars indicate standard error of the mean (n = 6 of LPS, n = 3 of VSV day 1 and n = 2 of VSV day 3).

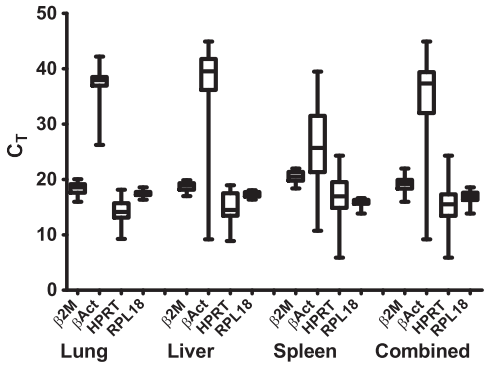

Fig. 2. Distribution of C_T values of the internal control genes in treated and untreated hamster tissues. Ribosomal protein L18 (RPL18) has the lowest variation between treated and untreated hamsters, followed by β-2-microglobulin (β2M), Hypoxanthine–guanine phosphoribosyltransferase (HPRT) and β-actin (βAct). The boxes indicate the 25th percentile to 75th percentile values, the middle line is the median value and the whiskers the total range of the values (n = 17 per tissue, n = 51 combined).

hamster homologues (Fig. 1A, Table 2 top panel). Additional problems with the ELISA results are the unusually high (roughly 1000-fold higher than to be expected) levels of TGFβ1 detected in comparison to mice. Therefore, we concluded that the tested ELISA kits are unreliable and of limited use for monitoring proteins involved in immune responses of hamsters. Similarly, the luminex rat and mouse panel data suggests that of the 55 different proteins tested only mouse IL-13 and MIG, and rat GM-CSF, IL-1α, Leptin and GRO/KC were detected with confidence in hamster plasma (Fig. 1B, Table 2 bottom panel). In addition, mouse Eotaxin, MIP-1β and IL-12 p40 as well as rat RANTES and IL-10 showed weak cross-reactivity for hamster proteins (Fig. 1C). All other cytokine analyses failed to show values above the limit of detection. These data suggest that, as with the ELISA kits, the tested luminex panels for rat and mouse cytokines/chemokines, with the exception of the six mentioned previously, are unreliable for the detection of immune responses in hamsters.

3.2. Gene data mining and selection

Given the limited cross-reactivity (Table 2) and high costs of mouse and/or rat ELISA and luminex based assays, qRT-PCR assays were considered and selected as the most practical detection system of choice to analyze hamster immune responses until further genome sequences become available. For this we analyzed specific hamster sequences registered on Genbank. Of the ~800 sequences available, 51 hamster specific genes involved in pro-inflammatory, anti-inflammatory, innate immunity, apoptosis, cell junction and coagulation responses, and four constitutively expressed reference genes were selected and TaqMan based qRT-PCR assays developed (Table 3).

3.3. Evaluation of internal reference genes

The identification of a suitable reference gene was of paramount importance for the assay development. Studies focusing on human tissues previously concluded that commonly used reference genes such as HPRT and β-actin may not be suitable as internal references due to large variations in expression between tissues and in responses to stresses (Dheda et al., 2004). Hamsters are outbred animals and therefore variability is inherent between individual animals. This makes selection of an appropriate internal reference critical (Dheda et al., 2004). β-actin, β2M, HPRT, and RPL18 were selected as potential housekeeping genes and individually evaluated for their expression levels in lung, liver and spleen tissues of treated/infected and control hamsters (n = 17 per tissue, n = 51 total). Fig. 2 shows the distribution of the fluorescence curves within representative tissues of infected, treated and untreated hamster tissues. β2M and RPL18 vary less than HPRT and β-actin (β2M standard deviation (SD) ≤ 1 cycle within tissues, 1.29 cycles between all samples; RPL18 SD ≤ 0.5 cycles within tissues, 0.87 cycles between all samples; HPRT SD ≤ 4.6 cycles within tissues, 3.4 cycles between all samples; β-actin SD ≤ 7.2 cycles within tissues, 7.5 cycles between all samples). Though previous work in hamsters has used HPRT and β-actin as reference genes (Melby et al., 1998; Muller et al., 2001; Vernel-Pauillac and Merien, 2006), in this study these internal reference

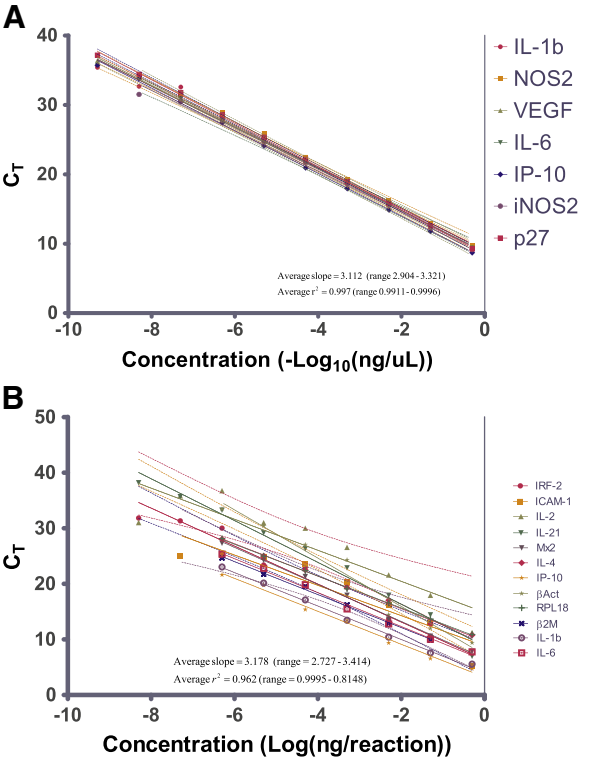

Fig. 3. Representative standard curve slope results for hamster qRT-PCR assays. Standard curves for selected assays were generated using (A) sequence specific plasmids as template (n = 15) and (B) sequence specific *in vitro* transcribed RNA as template (n = 12). Solid lines are the best fit curve and dashed lines represent the 95% confidence interval of the linear regression analysis. IL = Interleukin, IP-10 = Chemokine (C-X-C motif) ligand 10, NOS = Nitric Oxide Synthase, iNOS = inducible NOS, VEGF = Vascular Endothelial Growth Factor, p27 = Interferon α inducible protein p27, IRF = Interferon Regulatory Factor, ICAM = Intercellular Adhesion Molecule, Mx = myxovirus resistance protein, RPL18 = ribosomal protein L18, β2M = β-2-microglobulin, and βAct = β actin.

genes showed some variation between infected/treated and untreated hamsters and in comparison of different tissues (Fig. 2). The variation of β2M and, especially, RPL18 was much less in all instances. Therefore we chose to use RPL18 as the most reliable internal reference gene and propose that it should be strongly considered for future work.

3.4. Primer/probe efficiency and limit of detection

The average efficiency or E value of the primers was determined to be 3.112 (range 2.904–3.321, n = 15,) (Fig. 3A), *i.e.* 3.112 cycles per $\log_{10}$ dilution, when used on DNA template and 3.178 (range 2.727–3.414, n = 12) (Fig. 3B), *i.e.* 3.178 cycles per $\log_{10}$ dilution, when used on RNA template. The average r^2 values of the slopes were determined to be 0.9969 (range 0.9911–0.9996) from the DNA template (Fig. 3A) and 0.9616 (range 0.8148–0.9995) (Fig. 3B) from the RNA template. The signal generated per target template between the control and reference primer/probe sets was considered to be comparable as the efficiencies of the primer/probe sets were within 10% of the average (Ling et al., 2008). The limit of detection for the assayed primer/probe sets was determined to be between 10^{-6} to 10^{-8} ng gene-specific RNA which corresponds to 9–900 copies of the target RNA. The lowest amount of total RNA which could be used in these sets of experiments was determined to be 50 ng/25 μL reaction. The advantage of the approach is the sheer number of available assays and the diverse aspects of the immune system that can be analyzed, as well as the low amount of RNA necessary to perform each of the assays. Together, this allows for detailed analysis of several important genes even with lower RNA isolation yields.

3.5. Target RNA levels following LPS treatment

Previous studies using hamsters as a sepsis model reported complete fatality within three days post inoculation of *E. coli* (Steinwald et al., 1999). Hamsters used in our study developed severe "sepsis-like" symptoms (lethargy, ruffled fur, hunched posture and labored breathing) within one day following LPS treatment (50 μg) and were therefore euthanized and their tissues harvested. Hamster immune modulation was studied in selected tissues on day 1 post treatment (Fig. 4). The expression of pro-inflammatory genes was up-regulated with high transcript levels detected in the spleens and livers of the treated animals. Up-regulation of pro-inflammatory gene expression was less pronounced in lung tissue. Anti-inflammatory and immunoregulatory genes were up-regulated in all three tissues examined with liver being the strongest. The cell regulatory response was enhanced in

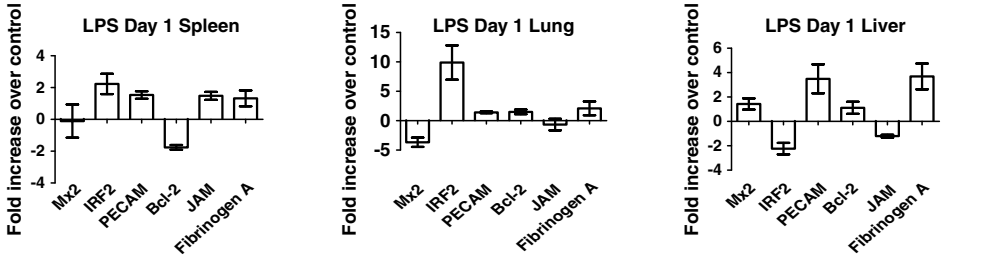

	LPS Day 1				LPS Day 1		
Pro-inflammatory, chemotaxis and T cell activation	Spleen	Lung	Liver	Anti-inflammatory and immunoregulatory	Spleen	Lung	Liver
Interleukin (IL-) 1β				IL-4			
IL-2				IL-10			
IL-2 receptor α				Forkhead box P3 (FoxP3)			
IL-6				IRF2			
IL-6 transducer				Transforming growth factor (TGF) β			
IL-12p35				TGFβ2			
IL-12p40				TGFβ3			
IL-21				TGFβ type I receptor			
Chemokine (C-X-C motif) ligand 10 (IP-10)				MHC class II antigen α antigen			
Intercellular adhesion molecule (ICAM) 1				Pro-apoptotic and cell regulatory			
Signal transducer and activator of transcription (STAT) 1				B-cell lymphoma 2 protein (Bcl-2) associated protein (bax)			
STAT-1β				Platelet endothelial cell adhesion molecule (PECAM)			
STAT2				Anti-apoptotic			
Interferon (IFN) γ				Bcl-2			
Interferon regulatory factor (IRF) 1				Cell junction integrity			
Tumor necrosis factor (TNF) α				E-cadherin			
p75 TNF membrane receptor				Tight junction protein			
Myxovirus resistance protein 2 (Mx2)				Junction adhesion molecule (JAM)			
Protein kinase R (PKR)				Claudulin-1			
IFNα inducible protein p27				Occuldin			
CD83 protein				Matrix metalloproteinase-2			
CCL20/MIP3-α				Tissue inhibitor of matrix metalloproteinase-2			
Nitric oxide synthase (NOS) 2				Clotting and Wound Healing			
Inducible NOS				Fibrinogen A α chain			
Complement C3d region				Vascular Growth			
Complement component 5				Vascular endothelial growth factor (VEGF)			
Complement component C1qBP							
Chemokine ligand 17							
Chemokine ligand 22							
Epithelial mucin (Muc1)							

>50-fold increase
20- to 50-fold increase
10- to 20-fold increase
5- to 10-fold increase
2- to 5-fol dincrease
<2-fold increase or decrease
2- to 5-fold decrease
5- to 10-fold decrease
10- to 20-fold decrease
20- to 50-fold decrease
>50-fold decrease

Fig. 4. Immune responses to LPS treatment in hamsters. Hamster immune gene expression profiles, with representative graphs (randomly selected), in spleen, lung and liver samples collected 1 day post-inoculation with 50 μg of LPS. Data is presented as fold increase over uninfected controls. Error bars indicate standard error of the mean (n = 6). For abbreviations see table in bottom part.

spleen and liver tissues, but the anti-apoptotic gene expression was unaltered in all three tissues. Cell junction and integrity responses appeared to be minimally altered in the spleen, increased in the lung and nearly unaffected in the liver in response to LPS treatment and the expression level of vascular endothelial growth factor (VEGF) was strongly decreased in the three tissues examined, suggesting a lack of endothelial cell proliferation (Ferrara and Davis-Smyth, 1997). A previous study focusing on LPS induced sepsis in the hamster model noted that liver and spleen showed higher levels of gene expression than lung and other tissues (Muller et al., 2001). In our study here the responses to LPS inoculation were also more pronounced in liver and spleen than in lung tissue, suggesting a much greater impact on these organs.

3.6. Target RNA levels following VSV infection

Hamsters are especially susceptible to VSV infection. Previous studies report that, in hamsters, as few as 10 pfu of VSV inoculated i.p. will result in uniform lethality within 72 h (Fultz et al., 1981a, 1981b). Upon infection with VSV (10^6 pfu) pro-inflammatory, innate and anti-inflammatory responses were largely up-regulated in all three organs examined with some being down-regulated (Fig. 5). Down- and up-regulation were especially pronounced in liver and spleen tissue (Fig. 5A and C). Pro-apoptotic genes were minimally up-regulated in expression in all tissues, but anti-apoptotic gene expression was increased only in the livers of infected animals. Expression of genes encoding for cell junction proteins was generally unaffected by VSV infection in liver, increased in the lungs, and reduced in the spleen of infected hamsters. Expression of fibrinogen was increased initially followed by a substantial decrease in expression in spleen and liver in final stages of the disease. This suggests that after infection with VSV there is a deregulation of cytokine and chemokine expression, which may precede or induce coagulation abnormalities in spleen and liver tissues of hamsters. Interestingly, the opposite was found for lung tissue (Fig. 5B). VEGF expression was strongly reduced in all

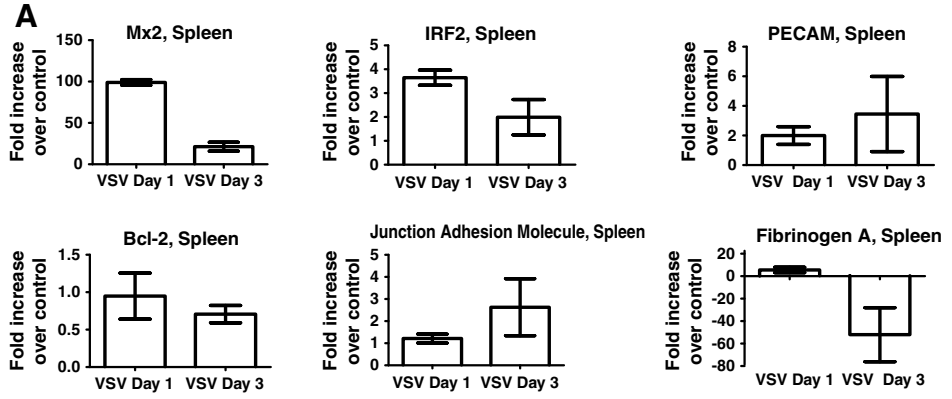

	Spleen			Spleen	
Pro-inflammatory, chemotaxis and T cell activation	Day 1	Day3	Anti-inflammatory and immunoregulatory	Day 1	Day 3
Interleukin (IL-) 1β			IL-4		
IL-2			IL-10		
IL-2 receptor α			Forkhead box P3 (FoxP3)		
IL-6			IRF2		
IL-6 transducer			Transforming growth factor (TGF) β		
IL-12p35			TGFβ2		
IL-12p40			TGFβ3		
IL-21			TGFβ type I receptor		
Chemokine (C-X-C motif) ligand 10 (IP-10)			MHC class II antigen α chain		
Intercellular adhesion molecule (ICAM) 1			Pro-apoptotic and cell regulatory		
Signal transducer and activator of transcription (STAT) 1			B-cell lymphoma 2 protein (Bcl-2) associated protein (bax)		
STAT-1β			Platelet endothelial cell adhesion molecule (PECAM)		
STAT2			Anti-apoptotic		
Interferon (IFN) γ			Bcl-2		
Interferon regulatory factor (IRF) 1			Cell junction integrity		
Tumor necrosis factor (TNF) α			E-cadherin		
p75 TNF membrane receptor			Tight junction protein		
Myxovirus resistance protein 2 (Mx2)			Junction adhesion molecule (JAM)		
Protein kinase R (PKR)			Claudulin-1		
IFNα inducible protein p27			Occuldin		
CD83 protein			Matrix metalloproteinase-2		
CCL20/MIP3-α			Tissue inhibitor of matrix metalloproteinase-2		
Nitric oxide synthase (NOS) 2			Clotting and wound healing		
Inducible NOS			Fibrinogen A α chain		
Complement C3d region			Vascular growth		
Complement component 5			Vascular endothelial growth factor (VEGF)		
Complement component C1qBP					
Chemokine ligand 17					
Chemokine ligand 22					
Epithlial mucin (Muc1)					

>50-fold increase
20- to 50-fold increase
10- to 20-fold increase
5- to 10-fold increase
2- to 5-fold increase
<2-fold increase or decrease
2- to 5-fold decrease
5- to 10-fold decrease
10- to 20-fold decrease
20- to 50-fold decrease
>50-fold decrease

Fig. 5. Immune responses to VSV infection in hamsters. Hamster immune gene expression profiles, with representative graphs (randomly selected), in (A) spleen, (B) lung and (C) liver collected at 1 and 3 days post infection with 10^6 pfu VSV. Data is presented as fold increase over uninfected controls. Error bars indicate standard error of the mean (n = 3 VSV day 1, n = 2 VSV day 3). For abbreviations see table in bottom part.

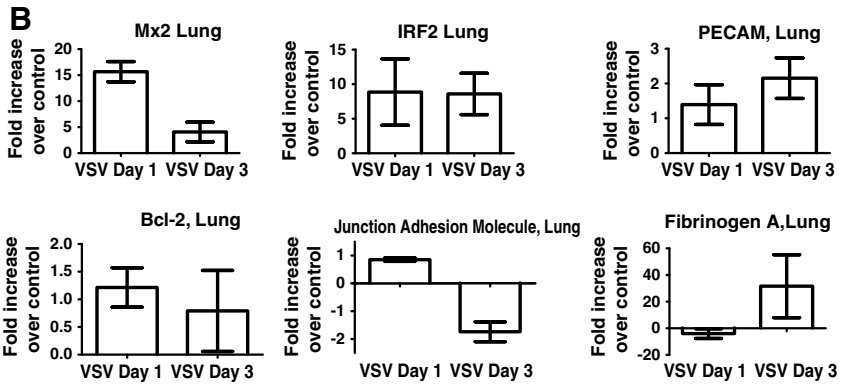

	Lung			Lung	
Pro-inflammatory, chemotaxis and T cell activation	Day 1	Day 3	Anti-inflammatory and immunoregulatory	Day 1	Day 3
Interleukin (IL-) 1β			IL-4		
IL-2			IL-10		
IL-2 receptor α			F		
IL-6			IRF2		
IL-6 transducer			Transforming growth factor (TGF) β		
IL-12p35			TGFβ2		
IL-12p40			TGFβ3		
IL-21			TGFβ type I receptor		
Chemokine (C-X-C motif) ligand 10 (IP-10)			MHC class II antigen α θchain		
Intercellular adhesion molecule (ICAM) 1			Pro-apoptotic and cell regulatory		
Signal transducer and activator of transcription (STAT) 1			B-cell lymphoma 2 protein (Bcl-2) associated protein (bax)		
STAT-1β			Platelet endothelial cell adhesion molecule (PECAM)		
STAT2			Anti-apoptotic		
Interferon (IFN) γ			Bcl-2		
Interferon regulatory factor (IRF) 1			Cell junction integrity		
Tumor necrosis factor (TNF) α			E-cadherin		
p75 TNF membrane receptor			Tight junction protein		
Myxovirus resistance protein 2 (Mx2)			Junction adhesion molecule (JAM)		
Protein kinase R (PKR)			Claudulin-1		
IFNα inducible protein p27			Occuldin		
CD83 protein			Matrixmetalloproteinase-2		
CCL20/MIP3-α			Tissue inhibitor of matrix metalloproteinase-2		
Nitric oxide synthase (NOS) 2			Clotting and wound healing		
Inducible NOS			Fibrinogen A α chain		
Complement C3d region			Vascular growth		
Complement component 5			Vascular endhelial growth factor (VEGF)		
Complement component C1qBP					
Chemokine ligand 17					
Chemokine ligand 22					
Epithelial mucin (Muc1)					

>50-fold increase
20- to 50-fold increase
10- to 20-fold increase
5- to 10-fold increase
2- to 5-fold increase
<2-fold increase or decrease
2- to 5-fold decrease
5- to 10-fold decrease
10- to 20-fold decrease
20- to 50-fold decrease
>50-fold decrease

Fig. 5 (*continued*).

tissues monitored during both early and terminal stages of infection. Overall the data imply that hamsters mount more robust immune responses in the liver and spleen than in the lung during VSV infection. Previous work identified the spleen and liver as the organs displaying pathological changes during VSV infection without notable involvement of the lungs, kidney, brain or intestinal tract (Fultz et al., 1981b). The similarities between our results and previous studies demonstrate the usefulness of our assays for more in depth evaluation of host responses to infection in an important animal model for which tools are largely lacking.

4. Conclusions

Mouse and rat ELISA and luminex panels tested in these studies were found to be of limited value for detecting hamster host responses. Instead, qRT-PCR assays for selected host response genes were established and validated on LPS-treated and VSV-infected hamsters. The assays allow for broad range monitoring of hamster immune and other cellular activities in host response to stress factors and the identification of RPL18 as an internal reference gene allows for accurate standardization. Thus, the developed assays will be instrumental in future applications of the hamster as a disease model until the full genome sequence is available allowing for the development of large scale RNA microarrays or deep sequencing.

Acknowledgements

The authors would like to thank Allen Grolla, Public Health Agency of Canada, Winnipeg, Canada, for help with the initial primer design and PCR; Katharine N. Bossart, Boston University, Boston, USA, for her fruitful discussion concerning realtime PCR; Gary Hettrick, Division of Intramural Research (DIR), National Institute of Allergy and Infectious Disease (NIAID), NIH, Hamilton, USA, for his help with visual graphics; and Joseph Prescott, DIR, NIAID, NIH, for his helpful suggestions regarding the manuscript. This work was supported by the Division of Intramural Research, National Institute of Allergy and Infectious Disease, National Institutes of Health.

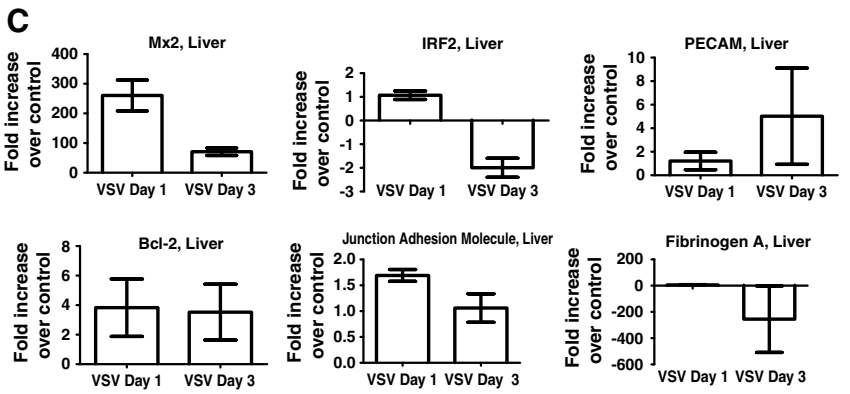

	Liver			Liver	
Pro-inflammatory, chemotaxis and T cell activation	Day 1	Day3	Anti-inflammatory and immunoregulatory	Day 1	Day 3
Interleukin (IL-) 1β			IL-4		
IL-2			IL-10		
IL-2 receptor α			Forkhead box P3 (FoxP3)		
IL-6			IRF2		
IL-6 transducer			Transforming growth factor (TGF) β		
IL-12p35			TGFβ2		
IL-12p40			TGFβ3		
IL-21			TGFβ2 type I receptor		
Chemokine (C-X-C motif) ligand 10 (IP-10)			MHC class II antigen α chain		
Intercellular adhesion molecule (ICAM) 1			Pro-apoptotic and cell regulatory		
Signal transducer and activator of transcription (STAT) 1			B-cell lymphoma 2 protein (Bcl-2) associated protein (bax)		
STAT-1 β			Platelet endothelial cell adhesion molecule (PECAM)		
STAT2			Anti-apoptotic		
Interferon (IFN) γ			Bcl-2		
Interferon regulatory factor (IRF) 1			Cell junction integrity		
Tumor necrosis factor (TNF) α			E-cadherin		
p75 TNF membrane receptor			Tight junction protein		
Myxovirus resistance protein 2 (Mx2)			Junction adhesion molecule(JAM)		
Protein kinase R (PKR)			Claudulin-1		
IFNα inducible protein p27			Occuldin		
CD83 protein			Matrix metalloproteinase-2		
CCL20/MIP3-α			Tissue inhibitor of matrix metalloproteinase-2		
Nitric oxide synthase (NOS) 2			Clotting and wound healing		
Inducible NOS			Fibrinogen A α chain		
Complement C3d region			Vascular growth		
Complement component 5			Vascular end othelial growth factor (VEGF)		
Complement component C1qBP					
Chemokine ligand 17					
Chemokine ligand 22					
Epithlial mucin (Muc1)					

>50-fold increase
20- to 50-fold increase
10- to 20-fold increase
5- to 10-fold increase
2- to 5-fold increase
<2-fold increase or decrease
2- to 5-fold decrease
5- to 10-fold decrease
10- to 20-fold decrease
20- to 50-fold decrease
>50- fold decrease

Fig. 5 (*continued*).

References

Adler, R., 2008. Janeway's immunobiology. Choice: Current Reviews for Academic Libraries, 45, p. 1793.

Beekes, M., Baldauf, E., Diringer, H., 1996. Sequential appearance and accumulation of pathognomonic markers in the central nervous system of hamsters orally infected with scrapie. J. Gen. Virol. 77 (Pt 8), 1925.

Braga, W., Venasco, J., Willard, L., Moro, M.H., 2006. Ultrastructure of Babesia WA1 (Apicomplexa: Piroplasma) during infection of erythrocytes in a hamster model. J. Parasitol. 92, 1104.

Bruder, C.E., Yao, S., Larson, F., Camp, J.V., Tapp, R., McBrayer, A., Powers, N., Granda, W.V., Jonsson, C.B., 2010. Transcriptome sequencing and development of an expression microarray platform for the domestic ferret. BMC Genomics 11, 251.

Chabry, J., Priola, S.A., Wehrly, K., Nishio, J., Hope, J., Chesebro, B., 1999. Species-independent inhibition of abnormal prion protein (PrP) formation by a peptide containing a conserved PrP sequence. J. Virol. 73, 6245.

Datson, N.A., Morsink, M.C., Atanasova, S., Armstrong, V.W., Zischler, H., Schlumbohm, C., Dutilh, B.E., Huynen, M.A., Waegele, B., Ruepp, A., de Kloet, E.R., Fuchs, E., 2007. Development of the first marmoset-specific DNA microarray (EUMAMA): a new genetic tool for large-scale expression profiling in a non-human primate. BMC Genomics 8, 190.

Dheda, K., Huggett, J.F., Bustin, S.A., Johnson, M.A., Rook, G., Zumla, A., 2004. Validation of housekeeping genes for normalizing RNA expression in real-time PCR. Biotechniques 37, 112.

Ferrara, N., Davis-Smyth, T., 1997. The biology of vascular endothelial growth factor. Endocr. Rev. 18, 4.

Fisher, A.F., Tesh, R.B., Tonry, J., Guzman, H., Liu, D., Xiao, S.Y., 2003. Induction of severe disease in hamsters by two sandfly fever group viruses, Punta toro and Gabek Forest (Phlebovirus, Bunyaviridae), similar to that caused by Rift Valley fever virus. Am. J. Trop. Med. Hyg. 69, 269.

Fultz, P.N., Shadduck, J.A., Kang, C.Y., Streilein, J.W., 1981a. Genetic analysis of resistance to lethal infections of vesicular stomatitis virus in Syrian hamsters. Infect. Immun. 32, 1007.

Fultz, P.N., Shadduck, J.A., Kang, C.Y., Streilein, J.W., 1981b. Involvement of cells of hematopoietic origin in genetically determined resistance of Syrian hamsters to vesicular stomatitis virus. Infect. Immun. 34, 540.

Garbutt, M., Liebscher, R., Wahl-Jensen, V., Jones, S., Moller, P., Wagner, R., Volchkov, V., Klenk, H.D., Feldmann, H., Stroher, U., 2004. Properties of replication-competent vesicular stomatitis virus vectors expressing glycoproteins of filoviruses and arenaviruses. J. Virol. 78, 5458.

Ghadirian, E., Meerovitch, E., Hartmann, D.P., 1980. Protection against amebic liver abscess in hamsters by means of immunization with amebic antigen and some of its fractions. Am. J. Trop. Med. Hyg. 29, 779.

Haake, D.A., 2006. Hamster Model of Leptospirosis. Curr. Protoc. Microbiol. Chapter 12, Unit 12E 2.

Hooper, J.W., Larsen, T., Custer, D.M., Schmaljohn, C.S., 2001. A lethal disease model for hantavirus pulmonary syndrome. Virology 289, 6.

Ierna, M., Kerr, A., Scales, H., Berge, K., Griinari, M., 2010. Supplementation of diet with krill oil protects against experimental rheumatoid arthritis. BMC Musculoskelet. Disord. 11, 136.

Jackson, A.C., SenGupta, S.K., Smith, J.F., 1991. Pathogenesis of Venezuelan equine encephalitis virus infection in mice and hamsters. Vet. Pathol. 28, 410.

Kayo, T., Allison, D.B., Weindruch, R., Prolla, T.A., 2001. Influences of aging and caloric restriction on the transcriptional profile of skeletal muscle from rhesus monkeys. Proc. Natl Acad. Sci. USA 98, 5093.

Larson, E.W., Dominik, J.W., Slone, T.W., 1980. Aerosol stability and respiratory infectivity of japanese B encephalitis virus. Infect. Immun. 30, 397.

Lawson, N.D., Stillman, E.A., Whitt, M.A., Rose, J.K., 1995. Recombinant vesicular stomatitis viruses from DNA. Proc. Natl Acad. Sci. USA 92, 4477.

Ling, K.H., Hewitt, C.A., Kinkel, S.A., Smyth, G.K., Scott, H.S., 2008. High-throughput and complex gene expression validation using the Universal ProbeLibrary and the LightCycler® 480 System. Biochemical 2, 23.

Livak, K.J., Schmittgen, T.D., 2001. Analysis of relative gene expression data using real-time quantitative PCR and the 2(−Delta Delta C(T)) Method. Methods 25, 402.

Melby, P.C., Tryon, V.V., Chandrasekar, B., Freeman, G.L., 1998. Cloning of Syrian hamster (*Mesocricetus auratus*) cytokine cDNAs and analysis of cytokine mRNA expression in experimental visceral leishmaniasis. Infect. Immun. 66, 2135.

Melby, P.C., Chandrasekar, B., Zhao, W., Coe, J.E., 2001. The hamster as a model of human visceral leishmaniasis: progressive disease and impaired generation of nitric oxide in the face of a prominent Th1-like cytokine response. J. Immunol. 166, 1912.

Milazzo, M.L., Eyzaguirre, E.J., Molina, C.P., Fulhorst, C.F., 2002. Maporal viral infection in the Syrian golden hamster: a model of hantavirus pulmonary syndrome. J. Infect. Dis. 186, 1390.

Muller, B., White, J.C., Nylen, E.S., Snider, R.H., Becker, K.L., Habener, J.F., 2001. Ubiquitous expression of the calcitonin-i gene in multiple tissues in response to sepsis. J. Clin. Endocrinol. Metab. 86, 396.

Niklasson, B.S., Meadors, G.F., Peters, C.J., 1984. Active and passive immunization against Rift Valley fever virus infection in Syrian hamsters. Acta Pathol. Microbiol. Immunol. Scand. C 92, 197.

Paessler, S., Aguilar, P., Anishchenko, M., Wang, H.Q., Aronson, J., Campbell, G., Cararra, A.S., Weaver, S.C., 2004. The hamster as an animal model for eastern equine encephalitis — and its use in studies of virus entrance into the brain. J. Infect. Dis. 189, 2072.

Roberts, A., Vogel, L., Guarner, J., Hayes, N., Murphy, B., Zaki, S., Subbarao, K., 2005. Severe acute respiratory syndrome coronavirus infection of golden Syrian hamsters. J. Virol. 79, 503.

Sbrana, E., Mateo, R.I., Xiao, S.Y., Popov, V.L., Newman, P.C., Tesh, R.B., 2006. Clinical laboratory, virologic, and pathologic changes in hamsters experimentally infected with Pirital virus (Arenaviridae): a rodent model of Lassa fever. Am. J. Trop. Med. Hyg. 74, 1096.

Siirin, M.T., Duan, T., Lei, H., Guzman, H., da Rosa, A.P., Watts, D.M., Xiao, S.Y., Tesh, R.B., 2007. Chronic St. Louis encephalitis virus infection in the golden hamster (*Mesocricetus auratus*). Am. J. Trop. Med. Hyg. 76, 299.

Smee, D.F., Gilbert, J., Leonhardt, J.A., Barnett, B.B., Huggins, J.H., Sidwell, R.W., 1993. Treatment of lethal Pichinde virus infections in weanling LVG/Lak hamsters with ribavirin, ribamidine, selenazofurin, and ampligen. Antivir. Res. 20, 57.

Spencer, J.F., Sagartz, J.E., Wold, W.S., Toth, K., 2009. New pancreatic carcinoma model for studying oncolytic adenoviruses in the permissive Syrian hamster. Cancer Gene Ther. 16, 912.

Steinwald, P.M., Whang, K.T., Becker, K.L., Snider, R.H., Nylen, E.S., White, J.C., 1999. Elevated calcitonin precursor levels are related to mortality in an animal model of sepsis. Crit. Care 3, 11.

Tesh, R.B., Guzman, H., da Rosa, A.P., Vasconcelos, P.F., Dias, L.B., Bunnell, J.E., Zhang, H., Xiao, S.Y., 2001. Experimental yellow fever virus infection in the Golden Hamster (*Mesocricetus auratus*). I. Virologic, biochemical, and immunologic studies. J. Infect. Dis. 183, 1431.

Vernel-Pauillac, F., Merien, F., 2006. Proinflammatory and immunomodulatory cytokine mRNA time course profiles in hamsters infected with a virulent variant of Leptospira interrogans. Infect. Immun. 74, 4172.

Wong, K.T., Grosjean, I., Brisson, C., Blanquier, B., Fevre-Montange, M., Bernard, A., Loth, P., Georges-Courbot, M.C., Chevallier, M., Akaoka, H., Marianneau, P., Lam, S.K., Wild, T.F., Deubel, V., 2003. A golden hamster model for human acute Nipah virus infection. Am. J. Pathol. 163, 2127.

Xiao, S.Y., Guzman, H., Zhang, H., Travassos da Rosa, A.P., Tesh, R.B., 2001. West Nile virus infection in the golden hamster (*Mesocricetus auratus*): a model for West Nile encephalitis. Emerg. Infect. Dis. 7, 714.

Zlotnik, I., Peacock, S., Grant, D.P., Batter-Hatton, D., 1972. The pathogenesis of western equine encephalitis virus (W.E.E.) in adult hamsters with special reference to the long and short term effects on the C.N.S. of the attenuated clone 15 variant. Br. J. Exp. Pathol. 53, 59.